ChemMedChem

Research Article
doi.org/10.1002/cmdc.202200686

Chemistry Europe
European Chemical Societies Publishing

www.chemmedchem.org

Discovery of a Chemical Probe to Study Implications of BPTF Bromodomain Inhibition in Cellular and *in vivo* Experiments

Paola Martinelli,[a] Otmar Schaaf,[a] Andreas Mantoulidis,[a] Laetitia J. Martin,[a] Julian E. Fuchs,[a] Gerd Bader,[a] Andreas Gollner,[a] Bernhard Wolkerstorfer,[a] Catherine Rogers,[b, c] Esra Balıkçı,[b, c] Jesse J. Lipp,[a] Nikolai Mischerikow,[a] Sandra Doebel,[a] Thomas Gerstberger,[a] Wolfgang Sommergruber,[a] Kilian V. M. Huber,[b, c] and Jark Böttcher*[a]

The bromodomain and PHD-finger containing transcription factor (BPTF) is part of the nucleosome remodeling factor (NURF) complex and has been implicated in multiple cancer types. Here, we report the discovery of a potent and selective chemical probe targeting the bromodomain of BPTF with an attractive pharmacokinetic profile enabling cellular and *in vivo* experiments in mice. Microarray-based transcriptomics in presence of the probe in two lung cancer cell lines revealed only minor effects on the transcriptome. Profiling against a panel of cancer cell lines revealed that the antiproliferative effect does not correlate with BPTF dependency score in depletion screens. Both observations and the multi-domain architecture of BPTF suggest that depleting the protein by proteolysis targeting chimeras (PROTACs) could be a promising strategy to target cancer cell proliferation. We envision that the presented chemical probe and the related negative control will enable the research community to further explore scientific hypotheses with respect to BPTF bromodomain inhibition.

Introduction

Bromodomain-containing proteins recognize acetylated lysine, an epigenetic mark found on histone tails, and modulate gene expression through multiple mechanisms. They can function as transcriptional co-regulators, as scaffolding proteins for the assembly of larger complexes of transcription factors, or as chromatin remodelers acting through various catalytic functions.[1] The bromodomain and PHD-finger containing transcription factor (BPTF) is a component of the nucleosome remodeling factor (NURF) complex[2] and comprises one of the 61 bromodomains encoded in the human genome.[3] BPTF binds both acetylated lysine on histone H4, through its bromodomain, as well as di- and tri-methylated lysine 4 on histone H3, through its PHD fingers[4] (Figure 1a). BPTF is essential for early embryo development[5] and for the maintenance of adult stem cells of the mammary gland[6] and the hematopoietic system.[7] Additionally, it has been implicated in multiple cancer types, including melanoma,[8] bladder cancer,[9] glioma,[10] and B-cell lymphomas.[11] The underlying mechanisms are likely diverse. For example, BPTF is required for the full activation of the MYC-dependent transcriptional program in MYC-driven lymphomas and pancreatic cancer models.[12] Others have suggested that BPTF can modulate tumor cell immunogenicity by regulating the antigen processing machinery.[13] A highly specific chemical probe would support the research community to unravel the complex role of BPTF in physiological and pathological processes.

Well-characterized chemical probes are valuable tools to analyze the effects of inhibiting protein interactions and/or enzymatic functions in cells and *in-vivo*.[14] Pioneer and prime example for the potential impact of a high quality chemical probe on the research community is the BET bromodomain inhibitor JQ1,[15,16] which enabled the later advancement of several compounds to human clinical trials[17]. Based on this success, increasing efforts to identify chemical probes for non-BET bromodomains have been initiated, leading to coverage of about half of the human bromodomain family.[18] Two respective probes are available for the BPTF bromodomain, which fulfill the stringent criteria set by the research community.[19] The data for the dual CECR2/BPTF probe and the BPTF probe

[a] Dr. P. Martinelli, Dr. O. Schaaf, Dr. A. Mantoulidis, Dr. L. J. Martin, Dr. J. E. Fuchs, Dr. G. Bader, Dr. A. Gollner, B. Wolkerstorfer, Dr. J. J. Lipp, Dr. N. Mischerikow, S. Doebel, Dr. T. Gerstberger, Dr. W. Sommergruber, Dr. J. Böttcher
Boehringer Ingelheim RCV GmbH & Co KG
Doktor-Boehringer-Gasse 5–11, 1120 Vienna (Austria)
E-mail: jark.boettcher@boehringer-ingelheim.com
[b] Dr. C. Rogers, Dr. E. Balıkçı, Dr. K. V. M. Huber
Target Discovery Institute
Nuffield Department of Medicine
University of Oxford, OX3 7FZ Oxford (UK)
[c] Dr. C. Rogers, Dr. E. Balıkçı, Dr. K. V. M. Huber
Centre for Medicines Discovery
Nuffield Department of Medicine
University of Oxford, OX3 7FZ Oxford (UK)

Supporting information for this article is available on the WWW under https://doi.org/10.1002/cmdc.202200686

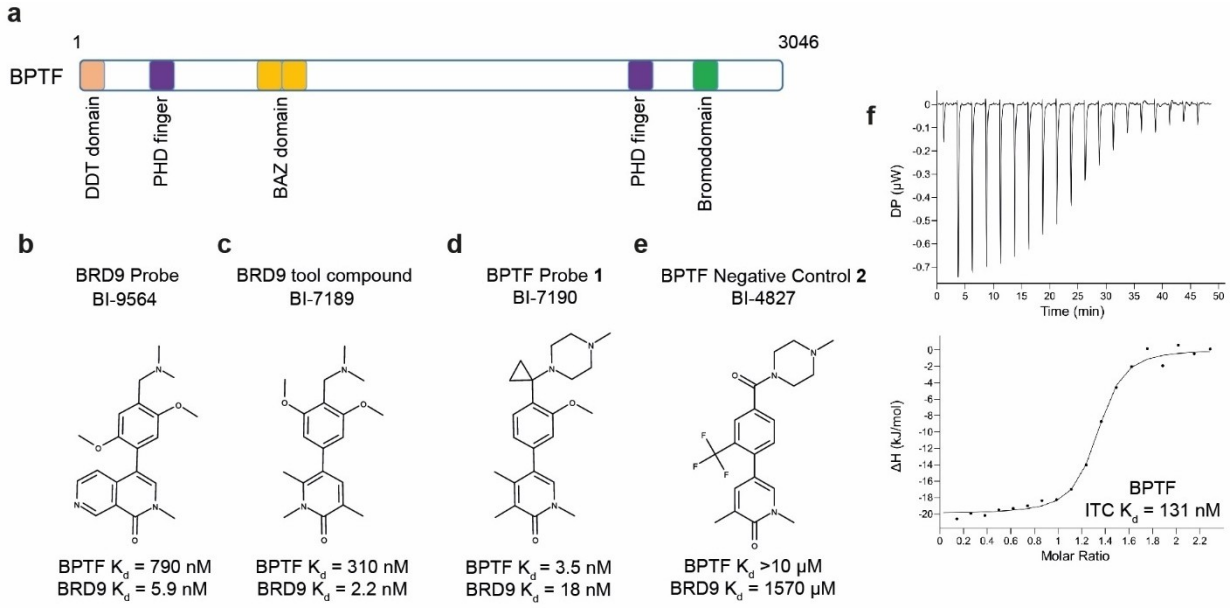

Figure 1. (**a**) Schematic representation of the domain architecture of the BPTF (Bromodomain PHD Finger Transcription Factor) protein (**b**–**e**) Chemical structures of and affinity data obtained by using the DiscoveRx BROMOscan platform. Data for (**b**) BRD9 Probe BI-9564 and (**c**) BRD9 tool compound BI-7189 have been reported previously. Data for (**d**) BPTF probe **1** and (**e**) BPFT negative control compound **2** are reported as mean of 3 independent experiments (in duplicates) ± standard deviations (shown in Table 1) (**f**) Isothermal titration calorimetry analysis of **2** ($K_d = 131 \pm 24$ nM; $\Delta H = -20.1$ kcal mol^{-1}; $\Delta G = -39.1$ kcal mol^{-1}; $-T\Delta S = -19.0$ kcal mol^{-1}); DP, measured power differential.

NVS-BPTF-1 have been made available prior to publication on the website of the Structural Genomics Consortium (https://www.thesgc.org/chemical-probes). Synthesis and biological evaluation of the latter one has been published in a separate study recently.[20] The probes are described as potent and selective inhibitors for cellular studies, but unfavorable ADME properties hinder potential *in-vivo* experiments. Here, we set out to develop a chemical probe which is suitable for *in vivo* studies in mice.

Results

Discovery of the chemical probe BI-7190

While developing the chemical probe BI-9564 (BRD9 K_d = 5.9 nM), for the bromodomain of BRD9, the structure activity relationship of dimethylpyridones was explored (Figure 1b).[21] The substitution in 4 or 6 position of the pyridine core led to high selectivity against the BET family, which was rationalized with a preferred torsion between the pyridine anchor and the aromatic rings occupying the ZA channel. A tool compound of the same structural class, BI-7189 (BRD9 K_d = 2.2 nM, Figure 1c) was used in parallel to elucidate the dependency of myeloid leukemia cells to BRD9 bromodomain inhibition paired with a bromo-swap strategy.[22] Interestingly, both molecules exhibited weak off-target binding to the distal bromodomain family member BPTF (BI-9564: BPTF K_d = 790 nM; BI-7189: BPTF K_d = 310 nM). Based on this observation, and the desire to elucidate the role of the BPTF bromodomain, we set out to profile selected compounds of this structural class against BPTF and BRD9 using assays of the DiscoveRx Corp. BROMOscan platform. One of the selected compounds, **1** (BI-7190) (Figure 1d), addressing the ZA channel with a methoxy-phenyl ring substituted with a conformationally restricted cyclopropyl methylpiperazine, exhibited outstanding binding affinity for the BPTF bromodomain (BPTF $K_d = 3.5 \pm 2.8$ nM). Interestingly, this cyclopropyl methylpiperazine substituent decreased the affinity for BRD9 ($K_d = 18.4 \pm 7.6$ nM) opening an attractive selectivity window. Profiling of a very close analog **2** (BI-4827), exhibited very weak binding affinity to the bromodomains of both BPTF ($K_d > 10$ µM) and BRD9 ($K_d = 1570 \pm 310$ nM) and was selected as potential negative control compound (Figure 1e). The binding affinity and the bromodomain selectivity of **1** were consecutively confirmed with Isothermal Titration Calorimetry (ITC) (BPTF $K_d = 131 \pm 24$ nM, BRD9 $K_d = 810 \pm 200$ nM, BRD7 $K_d = 5720 \pm 1130$ nM, Figure 1f, and Supporting Information (SI) Figure 1). A parallel shift of the affinities determined by the BROMOscan platform and ITC measurements is observed, highlighting the importance of confirmation with cellular target engagement measurements. To rationalize the unexpected selectivity for BPTF on a structural basis, we subjected **1** to co-crystallization experiments.

Structural basis of the selectivity

Co-crystals of **1** in complex with the BPTF bromodomain (amino acids 2917–3037)[3], diffracted to 1.0 Å and contained one ligand bound monomer per asymmetric unit in space group $P2_1$.

Compound **1** binds as expected to the acetyl-lysine binding site of the BPTF bromodomain (Figure 2a, SI Table 1). The ligand is anchored deeply in the cavity via hydrogen bonding between the pyridone carbonyl to both Asn2881 side-chain as well as a conserved buried water network. The ligand's polarized N-methyl group interacts with the sulfur lone pairs on Cys2877 while the single aromatic CH on the pyridone is in contact with the backbone carbonyl of Pro2825. The rigid biaryl scaffold of the ligand positions a phenylene ring adjacent to the backbone CH of Pro2825 and the side-chain of Trp2824 leading to CH-π and edge-to-face π-π-interactions respectively (similar π-interactions to the corresponding Trp81 in BRD4 have been described earlier).[23] The cyclopropylene linkage imposes an almost orthogonal orientation of phenylene and piperazine ring plains allowing the L-shaped ligand to contact the solvent-exposed rim of the bromodomain binding pocket. The protonated piperazine binds to a strongly negatively charged region forming a direct salt bridge to Asp2834 and profiting from additional contacts between the positively polarized N-methyl group and Asp2831. The striking binding selectivity can be attributed to a combination of conformational rigidity and electrostatic complementarity specific to the BPTF binding site. Molecular mechanics and quantum mechanics based conformational explorations identify L-shaped conformations close to the bioactive ones as lowest energy conformations of **1**. In contrast, the negative control **2**, bearing an amide linkage instead of the cyclopropylene conformational lock adopts majorly different ligand shapes at low energy levels. In the binding site context, the positive charge carried by the piperazine ring of **1** is placed in a hot spot of negative partial charges in proximity to Asp2834 and Asp2831. Both residues correspond to neutral amino acids in BRD9 (Ile53/Thr50) which provides a molecular basis for the experimentally observed selectivity (Figure 2b).

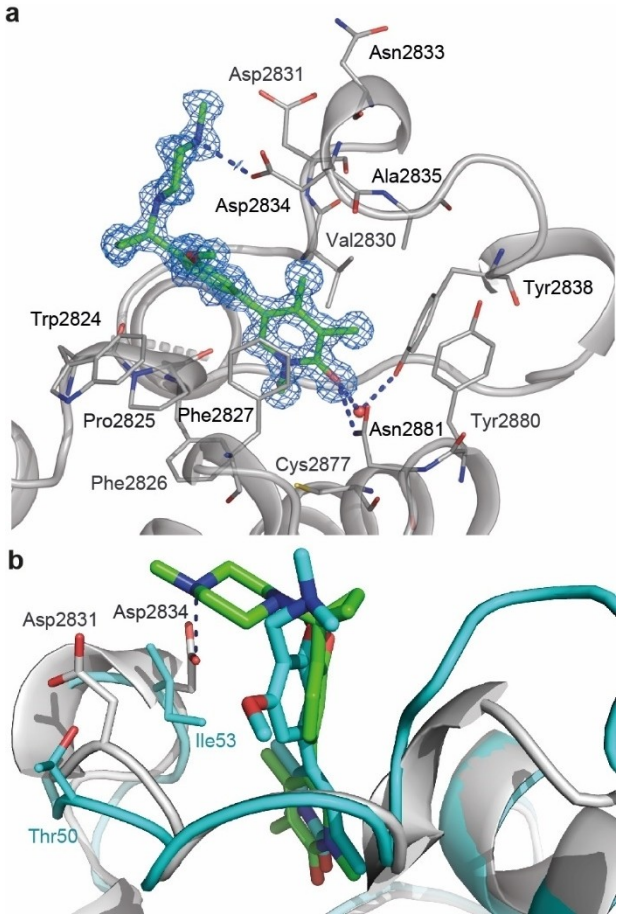

Figure 2. (**a**) Binding mode of **1** observed in the crystal structure in complex with the BPTF bromodomain$^{2917-3037}$ (pdb ID: 8AG2). **1** is shown as stick model, color coded by atom type with carbon shown in green. The refined $2F_o–F_c$ electron density shown in blue is contoured at 1.0 σ (**b**) Superposition of the crystal structure of compound **1** in BPTF and BRD9 in complex with BI-7189 (pdb ID: 8AHC) (C α r.m.s.d. 0.80 Å). **1** is shown as stick model, color coded by atom type with carbon shown in green and the respective BPTF protein is shown in grey, BI-7189 is shown as stick model, color coded by atom type with carbon shown in blue and the respective BPTF protein is shown in blue. Protein residues deemed important for selectivity are shown as sticks in the respective colors.

Characterization of the chemical probe BI-7190 for cellular experiments

Based on the attractive initial characteristics we decided to profile the probe **1** and the negative control **2** for potential off-targets, which could influence the cellular activity. In-class selectivity was assessed on a bromodomain panel (SI Table 2) and those targeted with $< 20\%$ ctrl at a concentration of 10 μM were subjected to K_d determination (SI Table 3). In addition to the known off-target BRD9, only three additional bromodomains showed significant inhibition with a binding affinity below 1 μM: BRD7 (close family member of BRD9), BRPF1 and CECR2 (K_d: BRD7 = 68.7 ± 25.7 nM; BRPF1 = 40.3 ± 18.8 nM; CECR2 = 390 ± 98 nM) and were nominated for further selectivity studies in cells. For a more general view on selectivity, we performed a kinase panel for **1** (SI Table 4) and a SafetyScreen44™ Panel for compound **1** and the negative control **2** (SI Table 5) suggesting no significant liabilities. To investigate the suitability of **1** as a cellular inhibitor of the BPTF bromodomain, cellular target engagement was determined using NanoBRET[24] (Figure 3a). The *in vitro* potency for BPTF translated into a potent BPTF cellular engagement (NanoBRET EC_{50} BPTF = 58 ± 40 nM), whereas the probe **1** showed only weak cellular target engagement against the off-target bromodomains and therefore revealing a sufficient cellular selectivity window with regard to other relevant bromodomain family members (NanoBRET EC_{50}: BRD9 = 1100 ± 250 nM; BRPF1 = 2960 ± 1690 nM; 13200 ± 6410 nM). As expected, the selected negative control **2** did not exhibit any relevant activity in the BPTF NanoBRET assay (Table 1, Figure 3a). Finally, the selectivity profile of **1** and its negative control **2** over a range of diverse targets was assessed. **1** was profiled in a kinase panel (SI Table 4) and a SafetyScreen44™ Panel (SI Table 5), and the negative control **2** was profiled in a SafetyScreen44™ Panel for (SI Table 5). No significant liabilities were identified for both compounds.

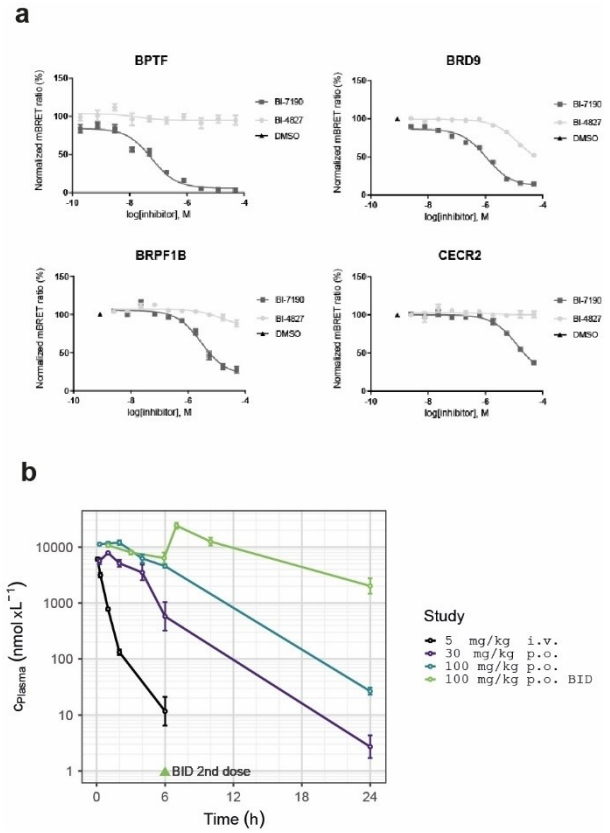

Figure 3. (**a**) Determination of cellular target engagement using NanoBRET; see Table 1 for a summary of EC_{50} values (**b**) In vivo pharmacokinetic profiles of **1** in C57BL/6 mouse plasma upon i.v. bolus and p.o. dosing. Data show mean values and standard deviations from n = 3 animals per dose group.

Characterization of the chemical probe BI-7190 for *in vivo* experiments

Favorable aqueous solubility, high absorptive permeability and low efflux ratio in the Caco-2 *in vitro* assay and low *in vitro* CYP450 inhibition suggested promising *in vivo* pharmacokinetic properties of **1** also for oral dosing (Table 1). Therefore, we assessed *in vivo* pharmacokinetic profiles in C57BL/6 mice. Despite the observation of relatively high plasma CL upon i.v. dosing, with doses of 30 and 100 mg/kg as single dose or 100 mg/kg bid, high plasma exposure and bioavailability were obtained upon oral dosing (Figure 3b and Table 1). Together with the moderate plasma protein binding and cellular target engagement at 58 nM, the favorable oral PK properties suggest **1** as a suitable tool compound for *in vivo* efficacy and mode-of-action studies.

Impact of BPTF bromodomain inhibition in cells

We tested the probe **1** on a panel of 46 cancer cell lines in a 7-day viability assay. The observed GI_{50} values ranged from 2.47 to 36.05 μM and did not correlate with either BPTF mRNA expression (source: CCLE) or the BPTF dependency score from two depletion screens[25,26] (Figure 4a). Cells from hematopoietic malignancies were slightly enriched among those with lower GI_{50} (SI Table 6 – not significant). Since chromatin remodeling is expected to modulate global transcription, we performed microarray-based transcriptomics in two cell lines, NCI-H1437 and NCI-H157, treated with **1** at a concentration of 1 μM over 120 h. Surprisingly, the treatment had only minor effects on the transcriptome. Principal component analysis revealed that most of the variation between samples could be ascribed to the time component (Figure 4b-left) likely reflecting confluency-dependent and nutrient availability-dependent transcriptional changes, while the treatment groups did not clearly separate (Figure 4b-right). Both cell lines behaved similarly (SI Figure 2a). When considering changes across time points, we found only three genes significantly modulated in NCI-H1437, namely *CLCF1*, *CLMP*, and *CLSPN*, while we did not observe any significantly modulated genes in NCI-H157 cells (Figure 4c and SI Figure 2b).

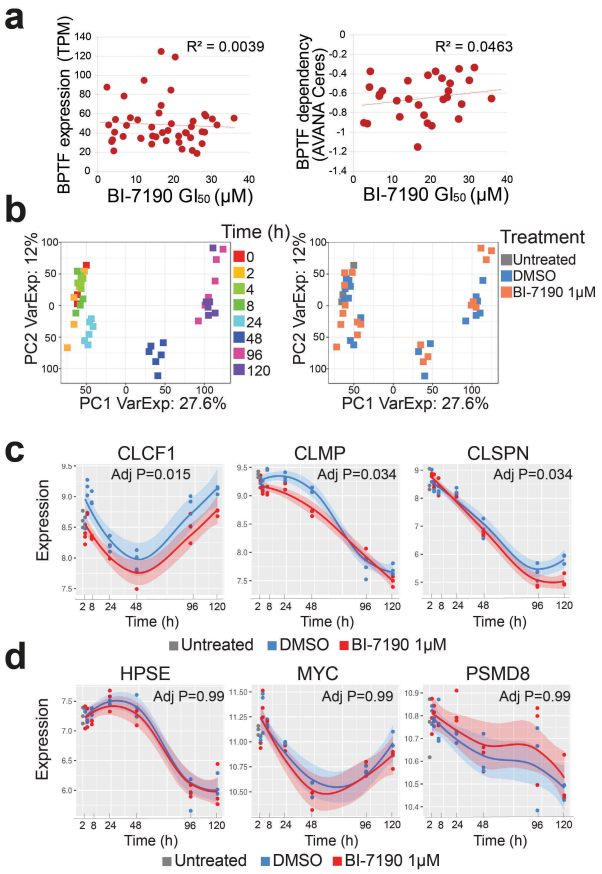

Figure 4. Treatment with BI-7190 induced minor transcriptional modulation in NCI-H1437 cells over 120 h. (**a**) Correlation of BI-7190 GI_{50} and BPTF expression (transcripts per million reads, TPM – left) or BPTF depletion score (from the AVANA depletion screen – right) Each dot represents one cell line tested. (**b**) Principal Component (PC) plots showing the variation among all samples analyzed in the transcriptomics experiment. Each dot represents one sample and dots are colored by time point (left) or treatment (right). The percentage of variation explained by the top two principal components is indicated in the axis labels. (**c**) Expression of the top differentially expressed genes over time in vehicle- or BI-7190-treated cells. Basal values in untreated cells are shown for reference. (**d**) Expression of the indicated BPTF targets as in (**c**).

Table 1. Summary and properties of BI-7190 and BI-4827. DiscoveRx K_d values are reported as mean of 3 independent experiments (in duplicates) ± standard deviations.

	Probe 1 BI-7190	Negative Control 2 BI-4827
BPTF-BD Affinity/Activity		
K_D(BPTF, DiscoveRx)	3.5 ± 2.8 nM	> 10 μM
K_D(BPTF, ITC)	131 ± 24 nM	n.d.
Bromodomain Selectivity		
K_D measurements for < 20% CTRL DiscoveRx at 10 μM/all other > 300 nM		
K_D(BRD9, DiscoveRx)	18.4 ± 7.6 nM	1570 ± 310
K_D(BRD7, DiscoveRx)	68.7 ± 25.7 nM	2833 ± 420
K_D(BRPF1, DiscoveRx)	40.3 ± 18.8 nM	> 10 μM
K_D(CECR2, DiscoveRx)	390 ± 98 nM	> 10 μM
Kinase Selectivity	No hits > 17%	n.d.
% ctrl inhibition at 10 μM		
Eurofins Cerep Safety Screen44™ Panel	No hits > 36%	No hits > 23%
% ctrl inhibition at 10 μM		
Target Engagement		
BPTF NanoBRET (EC_{50})	58 ± 40 nM	> 50000 nM
BRD9 NanoBRET (EC_{50})	1100 ± 250 nM	> 50000 nM
BRPF1 NanoBRET (EC_{50})	2960 ± 1690 nM	> 50000 nM
CECR2 NanoBRET (EC_{50})	13200 ± 6410 nM	> 50000 nM
In vitro ADME Properties		
Aqueous solubility (pH 6.8)	> 84 μg/ml	> 100 μg/ml
Hepatocytes pred. CL mouse/rat/human (% Q_H)	91/40/12	n.d.
Plasma protein binding mouse/rat/human (% bound)	61/48/59	n.d.
Human Cytochrome P450 inhibition IC_{50}	CYP2 C8: > 50 μM CYP2 C9: > 50 μM CYP2 C19: > 50 μM CYP2D6: > 50 μM CYP3 A4: 25 μM	n.d.
Caco-2 permeability $P_{app, a\text{-}b}$/efflux ratio	$54 \cdot 10^{-6}$ cm/s/1.5	n.d.
In vivo PK profile		
Mouse 5 mg/kg *i.v.* bolus plasma CL (% Q_H)/Vss	64/2.1 L/kg	n.d.
Mouse 30 mg/kg *p.o.* AUC(0-inf)/c_{max}/F_{oral}	33,200 nM·h/7.9 μM/145%	n.d.
Mouse 100 mg/kg *p.o.* AUC(0-inf)/c_{max}/F_{oral}	93,100 nM·h/13 μM/122%	n.d.
Mouse 100 mg/kg *p.o.* bid AUC(0-inf)/c_{max}/F_{oral}	241,000 nM·h/25 μM/158%	n.d.

No significant regulation was observed for the reported BPTF target genes *MYC*, *HPSE*, or *PSMD8*[13,27] (Figure 4d and SI Figure 2c).

We then focused on the top 50 genes showing some modulation over time, independent of the adjusted P value. As expected, probe **1** only induced minor changes in both cell lines and the modulated genes did not form obvious functional clusters (SI Figure 2d). However, the MYC-target *BUB1B*, which was shown to be reduced in *Bptf*-heterozygous Eμ-Myc lymphomas was slightly down-regulated in NCI-H1437 cells after 120 h treatment at 1 μM concentration (not significant – not shown).

Discussion

BPTF is a multidomain protein that has been implicated in multiple physiological and pathological processes, including various cancer types. Here we report the discovery of a chemical probe BI-7190, which is suitable to investigate the impact of chemical inhibition of the BPTF bromodomain in cells as well as *in vivo*. The probe, discovered within a structural class of BRD7/9 bromodomain inhibitors, was characterized with respect to *in vitro* target binding and possesses an attractive selectivity window towards other bromodomain family members. The translation of potency in a cellular context was confirmed using NanoBRET target engagement assays. Broader selectivity profiling outside of the protein family did not indicate any major off-target liabilities. The chemical probe displayed attractive *in vitro* and *in vivo* pharmacokinetic profiles, making it suitable for studies in both settings. *In vivo* studies might be particularly important to further investigate the proposed role of BPTF in tumor cell immunogenicity.

Despite its high affinity and selectivity for BPTF, the chemical probe had only a small effect on cell viability in a panel of cancer cell lines as well as on the global modulation of transcription in two cancer cell lines. Future studies might reveal similar or different effects in non-cancerous cells and tissues. Of note, BPTF binds acetylated histone tails also with its PHD finger, which is sufficient for the binding to nucleosomes[28] and interacts with transcription factors.[12] It is therefore possible that the inhibition of the bromodomain alone is not sufficient to fully abrogate all BPTF functions. This suggests that depleting BPTF by proteolysis targeting chimeras (PROTACs) could be a promising strategy to target cancer cell proliferation. A similar approach was successfully pursued for a significant number of bromodomain containing proteins.[29] Most prominent examples for this approach are SMARCA2/4 bromodomain inhibitor based PROTACs, whose targeted degradation phenocopied the anti-proliferative effects observed in genetic experiments[30] and BRD9 PROTACS, CFT8634 and FHD-609, in clinical

development.[31] In order to enable the research community to test scientific hypotheses with respect to BPTF bromodomain inhibition or prospective PROTAC approaches, we generated the chemical probe BI-7190 (**1**) and the related negative control BI-4827 **(2)**, which will be made available via EUbOPEN (EUbOPEN Chemical Probes (https://www.eubopen.org/chemical-probes)) as well as the Boehringer Ingelheim open innovation portal opnMe (BPTF inhibitor | BI-7190 | opnMe | Boehringer Ingelheim).

Methods

Protein purification

The construct for expression of BPTF protein (residues 2917–3037, UniProt ID: Q12830) containing a N-terminal GST-tag vector with TEV cleavage site is based on a previously reported structure.[3] The protein was expressed and purified as described in detail in the Supporting Information, concentrated to 3 mg/mL, and frozen at −80 °C.

Isothermal titration calorimetry

Calorimetric experiments of were performed on a MicroCal PEAQ-ITC instrument (Malvern Panalytical Ltd). Protein solutions were buffer exchanged by dialysis into buffer 25 mM HEPES pH 7.4, 150 mM Sodium Chloride and 1 mM TCEP. All measurements were carried out at 23 °C. Titrand and titrator concentrations were adjusted to 3% DMSO. The cell was loaded with protein solutions in the range of 0 to 25 μM. All injections were performed using an initial injection of 0.5 μL followed by 19 injections of 2 μL of compound in the range of 180–400 μM. The data were analyzed with the MicroCal PEAQ-ITC analysis software package (v1.1.0.1262). The first data point was excluded from the analysis. Thermodynamic parameters were calculated according to the Gibbs-Helmholtz equation ($\Delta G = \Delta H - T\Delta S = -RT\ln K_d$).

Protein crystallography

Crystals of the BPTF bromodomain (amino acids 2917–3037 of UniProt ID: P129830) were obtained using the sitting drop vapor diffusion method. At 4 °C 0.2 μl protein solution (8 mg/ml protein, concentrated after addition of 1 mM **compound 1**) were mixed with 0.14 μl reservoir solution containing 20% PEG 1000, 100 mM sodium cacodylate pH 6.5 and 0.2 M Magnesium chloride. Rod-like crystals grew to a final length of about 300 μm within 2 days. Crystals were flash-frozen in liquid nitrogen using reservoir solution supplemented with 35% PEG 400. Diffraction data was collected at beamline X10SA of the Swiss Light Source (Paul Scherrer Institute, Switzerland). Images were processed with autoPROC[32] and resolution limits were determined using default settings of autoPROC and STARANISO. The structure was solved by molecular replacement using the previously solved structure (PDB ID: 5R4O) as search model. The crystal structure of BI-7189 in complex with BRD9 was obtained as previously described. Model building and refinement was performed using standard protocols using CCP4,[33] COOT[34] and autoBUSTER (http://www.globalphasing.com). Statistics for data collection and refinement can be found in SI Table 1.

NanoBRET

HEK293 cells (4×10^5) were plated in 6-well plates and transfected with NanoLuc-BPTF ((NM_182641), BRD domain amino acids 2805–2905, cloned into pNLF1-N [CMV/Hygro] (Promega)), NanoLuc-BRPF1B, NanoLuc-BRD9, or NanoLuc-CECR2 (Promega), respectively. Twenty hours after transfection cells were collected, washed with PBS, and exchanged into OptiMEM I Reduced Serum Medium, no phenol red (ThermoFisher Scientific). Cell density was adjusted to 2×10^5 cells/ml and cells were re-plated in white 384-well polypropylene plates (Ultracruz). For BPTF, the in-house developed energy transfer probe (ETF) 5961 (https://www.thesgc.org/chemical-probes/NVS-BPTF-1, to be published) was added at a final concentration of 1 μM and for the remaining targets, NanoBRET ETF BRD_02 (Promega) was added at final concentrations of 0.2 or 1 μM, respectively. DMSO was added to each assay as control (no ETF control). **1** and **2** were then added directly to the wells at final concentrations starting from 50 μM and the plate was incubated for 2 h at 37 °C/5% CO_2. To measure BRET, NanoBRET furimazine substrate (Promega) and Extracellular NanoLuc Inhibitor (Promega) were added at final concentrations of 10 and 5 μM, respectively. Readings were performed within 10 min using a PHERAstar FSX (BMG LABTECH) equipped with a 460 nm BP filter (donor) and 618 nm LP filter (acceptor), with a 0.5 s reading setting. A corrected BRET ratio was calculated and defined as the ratio of the emission at 618 nm/460 nm for experimental samples (i.e. those treated with ETF) and the emission at 618 nm/460 nm for control samples (DMSO controls, not treated with ETF). BRET ratios are expressed as milli-BRET units (mBU), where 1 mBU corresponds to the corrected BRET ratio multiplied by 1000. Apparent EC_{50} values were determined for each test compound using Prism (GraphPad) assuming a sigmoidal dose-response (variable slope).

Cell lines

All cell lines were acquired from ATCC and periodic STR analysis and mycoplasma PCR testing were performed. Cells were cultured under standard conditions (37 °C, 5% CO_2, 20% O_2) according to the ATCC recommendations.

Cell viability assay

Cells were plated at low density in 384-well plates (500–1000 cells/well) and compounds were added on the next day. Cell viability was measured after 7 days with CellTiter-Glo luminescence system (Promega) following the manufacturer's instructions. Luminescence was measured in an Envision Plate Reader.

Microarray analysis

We measured time-resolved gene expression at 0, 2, 4, 8, 24, 48, 72, and 120 hours in untreated and BI-7190 treated cells (NCI-H1437 and NCI-H157) with three replicates per condition using Clariom™ S human microarrays. Data processing, analysis and visualization was done using the R programming language. After reading in the raw CEL files, we performed background correction and normalization using the Robust Multichip Average (RMA) algorithm provided by the "oligo" package[35] using standard parameters. As the data was acquired in two batches (replicate 1 versus replicates 2 and 3), we confirmed that RMA normalization was sufficient to remove any batch effects and that batch correction using "removeBatchEffect" from the "limma" package[36] did not have any additional beneficial effect. We used the "annotateEset" function from the "affycoretools" package to annotate the microarray probes with the information provided in the "p.clariom.s.human" package. Unannotated genes

and genes with low expression values were removed from the expression matrix. We defined contrasts between BI-7190-treated and untreated samples for each time point and identified differentially expressed genes using linear models followed by empirical Bayes correction as implemented in the "limma" package. Genes showing differential expression behavior over time were identified using limma's "topTableF" function. Raw p-values were corrected using the Benjamini-Hochberg method.

Chemical development

Synthesis and the respective characterization are reported in the Supporting Information. Reactions were carried out in standard commercially available glassware using standard synthetic chemistry methods unless stated otherwise. Reagents were obtained from commercial sources and used without additional purification.

Animal studies

In vivo pharmacokinetic studies in mice were carried out at WuXi AppTec (Shanghai) Co., Ltd under the animal ethics license PK-01-002-2017v1.2 (Institutional Committee Animal Care and Use Committee, Shanghai Site (IACUC-SH).

Disclaimer

This communication reflects the views of the authors and neither IMI nor the European Union, EFPIA or any Associated Partners are liable for any use that may be made of the information contained herein.

Acknowledgements

This project received funding from the Innovative Medicines Initiative 2 Joint Undertaking (JU) under grant agreement No 875510. The JU receives support from the European Union's Horizon 2020 research and innovation programme and EFPIA and Ontario Institute for Cancer Research, Royal Institution for the Advancement of Learning McGill University, Kungliga Tekniska Hoegskolan, Diamond Light Source Limited. We thank Steffen Steurer for upscaling of BI-7190, Moriz Mayer for compound analytics, Mark Pearson and Manfred Koegl for supervising biological experiments, Darryl B. McConnell for supervising medicinal chemistry.

Conflict of Interest

P. M., O. S., A. M., L. J. M., J. E. F., G. B., A. G., B. W., J. L., N. M., S. D., T. G., W. S., J. B. were full-time employees of Boehringer Ingelheim at the time this study was performed

Data Availability Statement

The authors declare that the data supporting the findings of this study have been deposited in the RCSB Protein Data Bank (PDB; http://www.rcsb.org) with the accession numbers 8AG2 (BPTF–BI-7190) and 8AHC (BRD9–BI-7189) or are available within the publication and its Supporting Information.

Keywords: BPTF · Bromodomain · Chemical Probes · Target2035 · EUbOPEN

[1] T. Fujisawa, P. Filippakopoulos, *Nat. Rev. Mol. Cell Biol.* **2017**, *18*, 246–262.
[2] H. Xiao, R. Sandaltzopoulos, H.-M. Wang, A. Hamiche, R. Ranallo, K.-M. Lee, D. Fu, C. Wu, *Mol. Cell* **2001**, *8*, 531–543.
[3] P. Filippakopoulos, S. Picaud, M. Mangos, T. Keates, J.-P. Lambert, D. Barsyte-Lovejoy, I. Felletar, R. Volkmer, S. Müller, T. Pawson, A.-C. Gingras, C. H. Arrowsmith, S. Knapp, *Cell* **2012**, *149*, 214–231.
[4] H. Li, S. Ilin, W. Wang, E. M. Duncan, J. Wysocka, C. D. Allis, D. J. Patel, *Nature* **2006**, *442*, 91–95.
[5] J. Landry, A. A. Sharov, Y. Piao, L. V. Sharova, H. Xiao, E. Southon, J. Matta, L. Tessarollo, Y. E. Zhang, M. S. H. Ko, M. R. Kuehn, T. P. Yamaguchi, C. Wu, *PLoS Genet.* **2008**, *4*, e1000241.
[6] W. D. Frey, A. Chaudhry, P. F. Slepicka, A. M. Ouellette, S. E. Kirberger, W. C. K. Pomerantz, G. J. Hannon, C. O. dos Santos, *Stem Cell Rep* **2017**, *9*, 23–31.
[7] B. Xu, L. Cai, J. M. Butler, D. Chen, X. Lu, D. F. Allison, R. Lu, S. Rafii, J. S. Parker, D. Zheng, G. G. Wang, *Stem Cell Rep* **2018**, *10*, 675–683.
[8] A. A. Dar, S. Majid, V. Bezrookove, B. Phan, S. Ursu, M. Nosrati, D. D. Semir, R. W. Sagebiel, J. R. Miller, R. Debs, J. E. Cleaver, M. Kashani-Sabet, *Proc National Acad Sci* **2016**, *113*, 6254–6258.
[9] C. Balbás-Martínez, A. Sagrera, E. Carrillo-de-Santa-Pau, J. Earl, M. Márquez, M. Vazquez, E. Lapi, F. Castro-Giner, S. Beltran, M. Bayés, A. Carrato, J. C. Cigudosa, O. Domínguez, M. Gut, J. Herranz, N. Juanpere, M. Kogevinas, X. Langa, E. López-Knowles, J. A. Lorente, J. Lloreta, D. G. Pisano, L. Richart, D. Rico, R. N. Salgado, A. Tardón, S. Chanock, S. Heath, A. Valencia, A. Losada, I. Gut, N. Malats, F. X. Real, *Nat. Genet.* **2013**, *45*, 1464–1469.
[10] A. L. Green, J. DeSisto, P. Flannery, R. Lemma, A. Knox, M. Lemieux, B. Sanford, R. O'Rourke, S. Ramkissoon, K. Jones, J. Perry, X. Hui, E. Moroze, I. Balakrishnan, A. F. O'Neill, K. Dunn, D. DeRyckere, E. Danis, A. Safadi, A. Gilani, B. Hubbell-Engler, Z. Nuss, J. M. M. Levy, N. Serkova, S. Venkataraman, D. K. Graham, N. Foreman, K. Ligon, K. Jones, A. L. Kung, R. Vibhakar, *Oncogene* **2020**, *39*, 2305–2327.
[11] L. Richart, I. Felipe, P. Delgado, M. P. de Andrés, J. Prieto, N. del Pozo, J. F. García, M. A. Piris, A. Ramiro, F. X. Real, *Oncogene* **2020**, *39*, 4884–4895.
[12] L. Richart, E. C. S. Pau, A. Río-Machín, M. P. de Andrés, J. C. Cigudosa, V. J. S.-A. Lobo, F. X. Real, *Nat. Commun.* **2016**, *7*, 10153.
[13] K. Mayes, S. G. Alkhatib, K. Peterson, A. Alhazmi, C. Song, V. Chan, T. Blevins, M. Roberts, C. I. Dumur, X.-Y. Wang, J. W. Landry, *Cancer Res.* **2016**, *76*, 6183–6192.
[14] C. H. Arrowsmith, J. E. Audia, C. Austin, J. Baell, J. Bennett, J. Blagg, C. Bountra, P. E. Brennan, P. J. Brown, M. E. Bunnage, C. Buser-Doepner, R. M. Campbell, A. J. Carter, P. Cohen, R. A. Copeland, B. Cravatt, J. L. Dahlin, D. Dhanak, A. M. Edwards, M. Frederiksen, S. V. Frye, N. Gray, C. E. Grimshaw, D. Hepworth, T. Howe, K. V. M. Huber, J. Jin, S. Knapp, J. D. Kotz, R. G. Kruger, D. Lowe, M. M. Mader, B. Marsden, A. Mueller-Fahrnow, S. Müller, R. C. O'Hagan, J. P. Overington, D. R. Owen, S. H. Rosenberg, B. Roth, B. Roth, R. Ross, M. Schapira, S. L. Schreiber, B. Shoichet, M. Sundström, G. Superti-Furga, J. Taunton, L. Toledo-Sherman, C. Walpole, M. A. Walters, T. M. Willson, P. Workman, R. N. Young, W. J. Zuercher, *Nat. Chem. Biol.* **2015**, *11*, 536–541.
[15] P. Filippakopoulos, J. Qi, S. Picaud, Y. Shen, W. B. Smith, O. Fedorov, E. M. Morse, T. Keates, T. T. Hickman, I. Felletar, M. Philpott, S. Munro, M. R. McKeown, Y. Wang, A. L. Christie, N. West, M. J. Cameron, B. Schwartz, T. D. Heightman, N. L. Thangue, C. A. French, O. Wiest, A. L. Kung, S. Knapp, J. E. Bradner, *Nature* **2010**, *468*, 1067–1073.
[16] A. R. Scott, *Nature* **2016**, *533*, S60–S61.

[17] A. G. Cochran, A. R. Conery, R. J. Sims, *Nat. Rev. Drug Discovery* **2019**, *18*, 609–628.
[18] M. A. Clegg, N. C. O. Tomkinson, R. K. Prinjha, P. G. Humphreys, *ChemMedChem* **2019**, *14*, 362–385.
[19] A. A. Antolin, P. Workman, B. Al-Lazikani, *Future Med. Chem.* **2021**, *13*, 731–747.
[20] L. Mélin, C. Calosing, O. A. Kharenko, H. C. Hansen, A. Gagnon, *Bioorg. Med. Chem. Lett.* **2021**, *47*, 128208.
[21] L. J. Martin, M. Koegl, G. Bader, X.-L. Cockcroft, O. Fedorov, D. Fiegen, T. Gerstberger, M. H. Hofmann, A. F. Hohmann, D. Kessler, S. Knapp, P. Knesl, S. Kornigg, S. Müller, H. Nar, C. Rogers, K. Rumpel, O. Schaaf, S. Steurer, C. Tallant, C. R. Vakoc, M. Zeeb, A. Zoephel, M. Pearson, G. Boehmelt, D. McConnell, *J. Med. Chem.* **2016**, *59*, 4462–4475.
[22] A. F. Hohmann, L. J. Martin, J. L. Minder, J.-S. Roe, J. Shi, S. Steurer, G. Bader, D. McConnell, M. Pearson, T. Gerstberger, T. Gottschamel, D. Thompson, Y. Suzuki, M. Koegl, C. R. Vakoc, *Nat. Chem. Biol.* **2016**, *12*, 672–679.
[23] G. Platzer, M. Mayer, A. Beier, S. Brüschweiler, J. E. Fuchs, H. Engelhardt, L. Geist, G. Bader, J. Schörghuber, R. Lichtenecker, B. Wolkerstorfer, D. Kessler, D. B. McConnell, R. Konrat, *Angew. Chem. Int. Ed. Engl.* **2020**, *59*, 14861–14868.
[24] T. Machleidt, C. C. Woodroofe, M. K. Schwinn, J. Méndez, M. B. Robers, K. Zimmerman, P. Otto, D. L. Daniels, T. A. Kirkland, K. V. Wood, *ACS Chem. Biol.* **2015**, *10*, 1797–1804.
[25] E. R. McDonald, A. de Weck, M. R. Schlabach, E. Billy, K. J. Mavrakis, G. R. Hoffman, D. Belur, D. Castelletti, E. Frias, K. Gampa, J. Golji, I. Kao, L. Li, P. Megel, T. A. Perkins, N. Ramadan, D. A. Ruddy, S. J. Silver, S. Sovath, M. Stump, O. Weber, R. Widmer, J. Yu, K. Yu, Y. Yue, D. Abramowski, E. Ackley, R. Barrett, J. Berger, J. L. Bernard, R. Billig, S. M. Brachmann, F. Buxton, R. Caothien, J. X. Caushi, F. S. Chung, M. Cortés-Cros, R. S. deBeaumont, C. Delaunay, A. Desplat, W. Duong, D. A. Dwoske, R. S. Eldridge, A. Farsidjani, F. Feng, J. Feng, D. Flemming, W. Forrester, G. G. Galli, Z. Gao, F. Gauter, V. Gibaja, K. Haas, M. Hattenberger, T. Hood, K. E. Hurov, Z. Jagani, M. Jenal, J. A. Johnson, M. D. Jones, A. Kapoor, J. Korn, J. Liu, Q. Liu, S. Liu, Y. Liu, A. T. Loo, K. J. Macchi, T. Martin, G. McAllister, A. Meyer, S. Mollé, R. A. Pagliarini, T. Phadke, B. Repko, T. Schouwey, F. Shanahan, Q. Shen, C. Stamm, C. Stephan, V. M. Stucke, R. Tiedt, M. Varadarajan, K. Venkatesan, A. C. Vitari, M. Wallroth, J. Weiler, J. Zhang, C. Mickanin, V. E. Myer, J. A. Porter, A. Lai, H. Bitter, E. Lees, N. Keen, A. Kauffmann, F. Stegmeier, F. Hofmann, T. Schmelzle, W. R. Sellers, *Cell* **2017**, *170*, 577–592.e10.
[26] R. M. Meyers, J. G. Bryan, J. M. McFarland, B. A. Weir, A. E. Sizemore, H. Xu, N. V. Dharia, P. G. Montgomery, G. S. Cowley, S. Pantel, A. Goodale, Y. Lee, L. D. Ali, G. Jiang, R. Lubonja, W. F. Harrington, M. Strickland, T. Wu, D. C. Hawes, V. A. Zhivich, M. R. Wyatt, Z. Kalani, J. J. Chang, M. Okamoto, K. Stegmaier, T. R. Golub, J. S. Boehm, F. Vazquez, D. E. Root, W. C. Hahn, A. Tsherniak, *Nat. Genet.* **2017**, *49*, 1779–1784.
[27] K. Mayes, Z. Elsayed, A. Alhazmi, M. Waters, S. G. Alkhatib, M. Roberts, C. Song, K. Peterson, V. Chan, N. Ailaney, P. Malapati, T. Blevins, B. Lisnić, C. I. Dumur, J. W. Landry, *Oncotarget* **2017**, *8*, 64344–64357.
[28] J. Wysocka, T. Swigut, H. Xiao, T. A. Milne, S. Y. Kwon, J. Landry, M. Kauer, A. J. Tackett, B. T. Chait, P. Badenhorst, C. Wu, C. D. Allis, *Nature* **2006**, *442*, 86–90.
[29] A. Vogelmann, D. Robaa, W. Sippl, M. Jung, *Curr. Opin. Chem. Biol.* **2020**, *57*, 8–16.
[30] W. Farnaby, M. Koegl, M. J. Roy, C. Whitworth, E. Diers, N. Trainor, D. Zollman, S. Steurer, J. Karolyi-Oezguer, C. Riedmueller, T. Gmaschitz, J. Wachter, C. Dank, M. Galant, B. Sharps, K. Rumpel, E. Traxler, T. Gerstberger, R. Schnitzer, O. Petermann, P. Greb, H. Weinstabl, G. Bader, A. Zoephel, A. Weiss-Puxbaum, K. Ehrenhöfer-Wölfer, S. Wöhrle, G. Boehmelt, J. Rinnenthal, H. Arnhof, N. Wiechens, M.-Y. Wu, T. Owen-Hughes, P. Ettmayer, M. Pearson, D. B. McConnell, A. Ciulli, *Nat. Chem. Biol.* **2019**, *15*, 672–680.
[31] A. Mullard, *Nat. Rev. Drug Discovery* **2021**, *20*, 247–250.
[32] C. Vonrhein, C. Flensburg, P. Keller, A. Sharff, O. Smart, W. Paciorek, T. Womack, G. Bricogne, *Acta Crystallogr. Sect. D* **2010**, *67*, 293–302.
[33] N. 4 C. C. Project, *Acta Crystallogr. Sect. D* **1994**, *50*, 760–3.
[34] P. Emsley, B. Lohkamp, W. G. Scott, K. Cowtan, *Acta Crystallogr. Sect. D* **2010**, *66*, 486–501.
[35] B. S. Carvalho, R. A. Irizarry, *Bioinformatics* **2010**, *26*, 2363–2367.
[36] M. E. Ritchie, B. Phipson, D. Wu, Y. Hu, C. W. Law, W. Shi, G. K. Smyth, *Nucleic Acids Res.* **2015**, *43*, e47–e47.

Manuscript received: December 16, 2022
Revised manuscript received: January 17, 2023
Accepted manuscript online: January 17, 2023
Version of record online: February 6, 2023